

Assessment of Submarine Groundwater Discharge (SGD) as a Source of Dissolved Radium and Nutrients to Moorea (French Polynesia) Coastal Waters

Karen L. Knee^{1,2} · Elizabeth D. Crook^{2,3} · James L. Hench⁴ · James J. Leichter⁵ · Adina Paytan²

Received: 20 January 2015 / Revised: 13 April 2016 / Accepted: 6 May 2016 / Published online: 3 June 2016
© Coastal and Estuarine Research Federation 2016

Abstract Previous work has documented large fluxes of freshwater and nutrients from submarine groundwater discharge (SGD) into the coastal waters of a few volcanic oceanic islands. However, on the majority of such islands, including Moorea (French Polynesia), SGD has not been studied. In this study, we used radium (Ra) isotopes and salinity to investigate SGD and associated nutrient inputs at five coastal sites and Paopao Bay on the north shore of Moorea. Ra activities were highest in coastal groundwater, intermediate in coastal ocean surface water, and lowest in offshore surface water, indicating that high-Ra groundwater was discharging into the coastal ocean. On average, groundwater nitrate and nitrite (N + N), phosphate, ammonium, and silica concentrations were 12, 21, 29, and 33 times greater, respectively, than those in coastal ocean surface water, suggesting that groundwater discharge could be an important source of nutrients to the coastal ocean. Ra and salinity mass

balances indicated that most or all SGD at these sites was saline and likely originated from a deeper, unsampled layer of Ra-enriched recirculated seawater. This high-salinity SGD may be less affected by terrestrial nutrient sources, such as fertilizer, sewage, and animal waste, compared to meteoric groundwater; however, nutrient-salinity trends indicate it may still have much higher concentrations of nitrate and phosphate than coastal receiving waters. Coastal ocean nutrient concentrations were virtually identical to those measured offshore, suggesting that nutrient subsidies from SGD are efficiently utilized.

Keywords Submarine groundwater discharge · Volcanic islands · Moorea · Nutrients · Radium

Introduction

Submarine groundwater discharge (SGD), commonly defined as any flow of groundwater (meteoric freshwater, recirculating seawater, or a mixture of the two) across the sediment-seawater interface (e.g., Burnett et al. 2001; Kim and Swarzenski 2010; Kim et al. 2011), is an important pathway by which terrestrial materials, including nutrients, metals, and various pollutants, are transported to the coastal ocean. Numerous studies have demonstrated that SGD can provide subsidies of freshwater (e.g., Garrison et al. 2003; Taniguchi et al. 2005; Knee et al. 2010), nutrients (Crotwell and Moore 2003; Garrison et al. 2003; Burnett et al. 2007) and metals (Basu et al. 2001; Montluçon and Sañudo-Wilhelmy 2001) that are comparable to or greater than those from river discharge or other sources. SGD is likely to be particularly important in areas with a steep seaward hydraulic gradient, high hydraulic conductivity, and little groundwater pumping, because these factors can increase the magnitude of seaward groundwater flow. Moreover, SGD has a greater relative importance in areas where river discharge

Communicated by Wayne S. Gardner

Electronic supplementary material The online version of this article (doi:10.1007/s12237-016-0108-y) contains supplementary material, which is available to authorized users.

✉ Karen L. Knee
knee@american.edu

¹ Department of Environmental Science, American University, Washington, DC, USA

² Institute of Marine Sciences, University of California, Santa Cruz, CA, USA

³ Department of Earth System Science, University of California, Irvine, CA, USA

⁴ Nicholas School of the Environment, Duke University, Beaufort, NC, USA

⁵ Scripps Institution of Oceanography, University of California, La Jolla, CA, USA

is low or nonexistent (e.g., Paytan et al. 2006; Shellenbarger et al. 2006; Knee et al. 2010).

The flux of SGD to the coastal ocean from volcanic oceanic islands is expected to be especially high for several reasons. Many of these islands are comprised of porous basalt (MacDonald et al. 1983; Won et al. 2006; Neall and Trewick 2008), which has a high hydraulic conductivity (Freeze and Cherry 1979). Many volcanic islands, including Moorea, have steep topography, which would generally correspond to a steep seaward hydraulic gradient in a shallow, unconfined aquifer. Islands with relatively low population densities, such as Moorea's 120 people per km² (ISPF 2015), and undeveloped, steep interior areas would generally have a lower proportion of land covered by impermeable surfaces compared to more developed continental coastal regions, facilitating groundwater recharge. Additionally, many islands, including the main Hawaiian Islands (Giambelluca et al. 2013) and Tahiti (Serafini et al. 2014), receive heavy orographic precipitation on their upper slopes. Moorea's latitudinal position in the Intertropical Convergence Zone also leads to strong seasonal variability in precipitation, with heavy rainfall occurring in the Austral summer. If some or all of this water becomes groundwater recharge, it would flow down gradient through the aquifer and eventually discharge at the coastline.

Indeed, previous studies have demonstrated that, on some volcanic oceanic islands, SGD contributes significant fluxes of freshwater, nutrients, and other dissolved constituents to coastal ocean waters. SGD on Jeju Island, in the southern Sea of Korea, ranged from 50 to 300 m³ y⁻¹ per m² of coastal seafloor (or m y⁻¹ when expressed as a seepage rate; Kim et al. 2003), and the nutrient subsidies it provided contributed to benthic eutrophication in Bangdu Bay (Hwang et al. 2005). Street et al. (2008) reported SGD fluxes of up to 237, 73, and 142 m³ per m² of coastal seafloor per year for the islands of Hawai'i, Maui, and Moloka'i, respectively. Similar fluxes were measured on the Kona coast of Hawai'i by Peterson et al. (2009) and Knee et al. (2010). Many oceanic volcanic islands support coral reefs (Table 1), which may be vulnerable to loading of nutrients and other pollutants by SGD. Where they have been quantified, SGD fluxes from oceanic volcanic islands to the surrounding fringing coral reefs have often been high (e.g., Senal et al. 2011; Povinec et al. 2012; Ji et al. 2013); however, on many volcanic islands, including Moorea, SGD has never been measured (Supplementary Material).

Coral reefs are sensitive to variations in water temperature, salinity and, at least under some circumstances, nutrient concentrations (Coles and Jokiel 1992; Jokiel 2004; Fabricius 2005), all of which can be affected by SGD. SGD often has a distinct temperature signature from ambient seawater,

sometimes enabling the delineation of SGD plumes via remote sensing (e.g., Duarte et al. 2006; Johnson et al. 2008). Fresh or brackish SGD lowers the salinity of coastal waters (e.g., Kroeger et al. 2007; Street et al. 2008; Knee et al. 2010). High concentrations of nutrients (nitrate, phosphate, and ammonium) in groundwater can be derived from fertilizer and manure use and onsite wastewater treatment (cesspools and septic systems), which are common in remote island locations with relatively low population densities and limited infrastructure. Excess nutrient loading has been linked to a number of deleterious effects on coral reefs, including coral disease (Bruno et al. 2003; Voss and Richardson 2006; Baker et al. 2007), and phase shifts to macroalgal-dominated reefs (McCook et al. 2001). SGD has been shown to be a source of new nitrogen to coral reefs in Florida, Hawai'i, Mauritius, the Gulf of Aqaba and Mexico (Paytan et al. 2006; Null et al. 2014). Pesticides, trace metals and microorganisms from agriculture and wastewater can also harm reefs (van Dam et al. 2011; Sutherland et al. 2011). Agricultural practices on Moorea include fertilizer and pesticide applications as well as raising livestock, and the population relies exclusively on septic systems for wastewater treatment (Boutillier and Duane 2006). Thus, discharge of polluted groundwater into the island's two large bays, Paopao Bay and Opunohu Bay, and other coastal waters could impact adjacent coral reefs.

Moorea's fringing and back reefs, which parallel the island's coastline approximately 500–1200 m from shore (Williams 1933), are sites of high productivity and biodiversity, supporting corals, algae, invertebrates, and fish. The island is also a hub of scientific research, mainly focused on coral reef ecology. The University of California, Berkeley, maintains the Richard B. Gump South Pacific Research Station, and the National Science Foundation supports a Long-Term Ecological Research (LTER) site there. Physical, chemical and biological parameters have been monitored regularly since the Moorea Coral Reef LTER site was established in 2004 (see <http://mcr.lternet.edu/>; Leichter et al. 2013). The French École Pratique de Hautes Etudes (EPHE) and National Center for Scientific Research (CNRS) also maintain a research station, the Centre de Recherches Insulaires et Observatoire de l'Environnement (Center for Island Research and Environmental Observatory; French acronym, CRIOBE) on Moorea. It is important to understand the quantity and quality of SGD in order to put long-term data being collected at these research stations in context, understand potential risks to the reefs from SGD-borne nutrients and contaminants and to aid in preserving the reef and island ecosystems.

To shed light on how SGD may affect coral reefs on Moorea and other volcanic islands, this study sought to (1) estimate the quantity of SGD to several sites on Moorea's

Table 1 List of volcanic oceanic islands with coral reefs where SGD has been quantified. Although SGD on these islands is likely to be high and to impact coral reef health, SGD has not been quantified on most volcanic islands with coral reefs worldwide (see [Supplementary Material](#))

Region	Country	Island or island group	Studies quantifying SGD	SGD ($\text{m}^3 \text{m}^{-1} \text{day}^{-1}$)		
Central Indian Ocean	Republic of Mauritius	Mauritius	Paytan et al. 2006	83–87		
			Povinec et al. 2012	35–220		
Southeast Asia	Philippines	Over 7000 islands	Taniguchi et al. 2008	12.4		
			Senal et al. 2011	210–480		
			Taiwan	Taiwan	Lin et al. 2011	616
			Japan	Okinawa	Blanco et al. 2011	0.2–0.3
			China	Hainan Island	Su et al. 2011	14.6–72.5
Australia and Oceania	United States	Guam	Matson 1993	13,200–28,100		
			Johnson 2012	2.2–110		
	France	Moorea (Society Islands)	This study		8.4	
			United States	Hawaiian archipelago	Garrison et al. 2003	115–527
	United States	Hawaiian archipelago	Paytan et al. 2006	6.43 (O'ahu)		
			Street et al. 2008	50–109 (Hawai'i), 35–114 (Maui)		
			Knee et al. 2008	0.75–925 (Hawai'i), 1–5.3 (Maui), 8.4–942 (Moloka'i)		
			Peterson et al. 2009	1.9–11.2 (Kaua'i)		
			Knee et al. 2010	1200 (Hawai'i)		
			Peterson et al. 2009	4.32–1870 (Hawai'i)		
			28–101 (Hawai'i)			

coast, (2) determine the contribution of SGD to Moorea's coastal salinity and nutrient budgets, and (3) compile data on SGD from other islands that support coral reefs in order to explore how SGD may affect these ecosystems worldwide.

Study Site

The island of Moorea is located in the Society Islands of French Polynesia ($17^{\circ} 30' \text{ S}$, $149^{\circ} 50' \text{ W}$), 20 km west of the larger island of Tahiti (Fig. 1). With a land area of 132 km^2 and a maximum elevation of 1207 m, it is classified as a small, volcanic high island. The island's climate is tropical with two distinct seasons: a cooler ($19\text{--}25^{\circ} \text{C}$), drier winter from May to November and a warmer ($21\text{--}29^{\circ} \text{C}$), wetter summer from December to April (Moorea Coral Reef LTER 2014). Since meteorological monitoring at the Moorea LTER site began in 2006, annual rainfall has ranged from 710 to 2560 mm, with a median value of 1240 mm (Washburn 2014). No rain was recorded during the study period in August 2008. The average annual evaporation rate during the period 1957–1986 at a monitoring station on Tahiti was 1683 mm (Pasturel 1993; Hildenbrand et al. 2005), and would likely be similar on Moorea since the two islands are located close together and have similar climates.

Streams on Moorea are small, and most only flow during the summer or after local rain events. The island's largest perennial river is the Opunohu, which flows into Opunohu Bay, to the west of Paopao Bay (Fig. 1). Smaller streams include two in the Teavaro District and the Vaioro River in the middle of the island's east coast (Resh et al. 1999). A seasonal stream discharges into the southern end of Paopao Bay. None of the island's streams is gauged or regularly monitored.

With the exception of Hawai'i, the hydrogeology and groundwater resources of most volcanic oceanic islands are poorly documented (Hildenbrand et al. 2005), and, to the best of our knowledge, no studies specifically focusing on Moorea's hydrogeology have been published. However, a study of nearby Tahiti documented freshwater springs discharging into rivers and directly into coastal waters, with the groundwater originating from both basal and perched aquifers. Most groundwater discharge from the basal aquifer occurred via a lateral discontinuity in the volcanic structure located on the seafloor beyond the barrier reef at a depth of 1000–1500 below sea level (Hildenbrand et al. 2005). Since the climate, rainfall and geology of Moorea and Tahiti are similar, it is reasonable to expect that a similar general pattern of groundwater flow would exist; however, the specific locations of dikes, landslides, discontinuities, and other geologic features

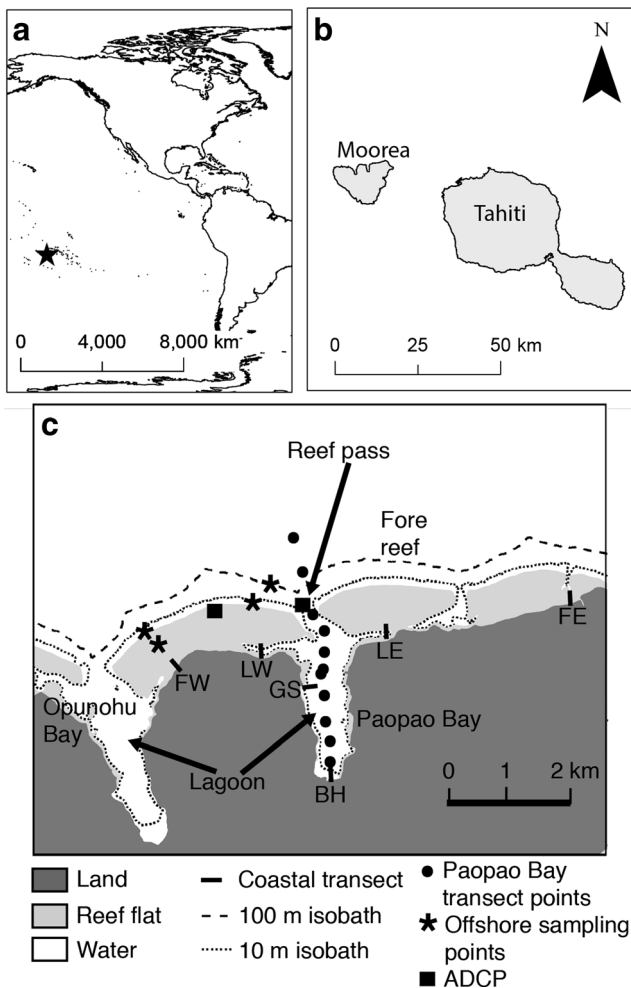


Fig. 1 Map of the study location showing **a** location of Moorea (indicated by a *star*) in the Pacific Ocean, **b** size and shape of Moorea and its larger neighbor, Tahiti, and **c** details of the study location. Approximate length and orientation of coastal ocean transects are indicated, but locations of individual sampling points (except in the longer Paopao Bay transect and offshore points) are not due to scale. Reef pass, fore reef, and lagoon features are present in both Paopao Bay and Opunohu Bay. The reef flat is depicted in a different color from deeper water and is generally 1–3 m deep with only the tops of the tallest corals emergent

would control the direction of groundwater flow and the locations of springs or areas of diffuse SGD.

Sampling was focused on Paopao Bay, also known as Cook's Bay, and adjacent sections of coastline (Fig. 1). Paopao Bay is separated from the offshore ocean by a barrier reef and a shallow back reef lagoon. A narrow (<100 m wide), relatively deep (50 m maximum depth) pass connects the back reef lagoon to the open ocean (Hench et al. 2008). Paopao Bay is one of 12 reef-lagoon-pass systems on Moorea, and it is typical of other high island reef systems with relatively large inshore bays (Leichter et al. 2013). The bay runs approximately north-south, is about 3 km long by 1 km wide, and has a mean depth of 25–30 m. Tidal amplitudes in this area are small

(about 0.15 m) and circulation is driven by offshore wave events as well as diurnal heat fluxes and episodic winds (Hench et al. 2008; Monismith et al. 2013; Herdman et al. 2015).

Methods

Field sampling was conducted from August 19 to August 23, 2008. We used a small boat to collect samples at 11 stations along a transect extending from the most inland part, or head, of Paopao Bay, near the town of Paopao, to 1 km offshore of the bay mouth (Fig. 1). We also collected samples along shorter coastal ocean transects at Paopao Bay head (BH) and five additional sites (Fig. 1) by wading. From West to East, the five sites were as follows: Reef Flat West (FW), Lagoon West (LW), Gump Station (GS), Lagoon East (LE), and Reef Flat East (FE). LW corresponds to the location of a long-term data site maintained by the Moorea LTER. Each coastal ocean transect was oriented perpendicular to the shoreline, extended from the shoreline to a depth of approximately 1.5 m and consisted of 4–6 sampling points. At each coastal ocean transect site, between 1 and 10 coastal groundwater samples were collected just inland (0.25–2 m) of wherever the land-water boundary was located at the time of sample collection. Groundwater samples were collected by excavating a beach pit to the water table and collecting the groundwater with a small submersible pump. One to 2 groundwater samples were collected at FW, LW, BH, and LE during a single sampling event, while at GS, a shore-perpendicular transect of 2–3 groundwater pits was sampled 4 times to capture variability driven by the daily tidal cycle. Additionally, a boat was used to collect 2 surface water samples 250 and 440 m offshore of FW (approximate water depth of 2 and 5 m, respectively, Fig. 1), 2 surface water samples from the lagoon and fore reef 1000 and 1500 m offshore of LW (approximate water depth = 2 and 15 m, respectively, Fig. 1), 6 samples in the vicinity of the FE site at distances of 0–100 m from shore, and one sample from the mouth of the ungauged stream discharging into Paopao Bay.

Activities of three radium isotopes (^{223}Ra , ^{224}Ra , and ^{228}Ra , with half lives of 11.4 d, 3.6 d, and 5.8 y, respectively), concentrations of nutrients (combined nitrate and nitrite or $\text{N} + \text{N}$, NH_4^+ , PO_4^{3-} , and SiO_2) and salinity were measured on each water sample, except that Ra isotope activities and salinity were not measured on samples from FE due to unexpected difficulties in the field. Groundwater and surface water Ra samples (generally 40 and 100 L per sample, respectively) were collected and analyzed following the procedures described by Null et al. (2012) using a RaDeCC delayed coincidence counter. Uncertainties associated with Ra isotope activities were determined following Garcia-Solsona et al. (2008) and averaged 38, 10, and 10% of sample activity for

^{223}Ra , ^{224}Ra , and ^{228}Ra , respectively. Nutrient samples were filtered in the field with a 0.45- μm filter, acidified to pH 2 with hydrochloric acid and stored until analysis in acid-washed polyethylene bottles. Nutrient concentrations were analyzed using a Lachat Quickchem Flow Injection Autoanalyzer at the University of California, Santa Cruz. Instrument error was <5 % for all nutrients based on duplicates analyzed every 10 samples. Water temperature and salinity were measured in the field using a YSI 85 hand-held meter. The maximum error associated with YSI measurements was 1 % for temperature and 2 % for salinity, according to the product manual.

We estimated submarine groundwater discharge (SGD) fluxes into coastal waters at each site where Ra isotope activities were measured (FW, LW, GS, BH, LE, and Paopao Bay) using a simple mass-balance approach (Eq. 1)

$$\text{SGD} = \frac{V_{\text{box}}(A_{\text{box}} - A_{\text{os}})}{T_r A_{\text{gw}}} \quad (1)$$

where SGD is a flux in $\text{m}^3 \text{day}^{-1}$; V_{box} is the volume of the coastal ocean box in m^3 ; A_{box} , A_{os} , and A_{gw} are the Ra activities of water within the coastal ocean “box” at each site, the off-shore ocean, and the groundwater endmember discharging into the coastal ocean at each site, respectively; and T_r is the residence time (days) of water in the coastal ocean box. For all short transects (FW, LW, GS, BH and LE; Fig. 1), A_{box} was estimated as the mean Ra activity of all coastal ocean samples collected within 100 m of the shoreline at that site. For Paopao Bay, A_{box} was the weighted average Ra isotope activity, with weights corresponding to the fraction of the total transect length represented by each measurement. A_{os} was the mean Ra activity of the 4 offshore samples collected 250–500 m from the shoreline at FW and 1000–1500 m from the shoreline at LW (Fig. 1). We note that the expression V_{box}/T_r in Eq. 1 is equivalent to water flow (Q , $\text{m}^3 \text{day}^{-1}$). Eq. 1 assumes that the groundwater sampled is responsible for most or all Ra enrichment in the coastal ocean and that other potential Ra sources, namely rivers and bottom sediments, are negligible Ra sources in comparison to SGD. For short coastal ocean transects (Fig. 1), the width of each box (corresponding to shoreline length) was 1 m, the average depth was 1 m, and the transect length was 50–75 m, resulting in box volumes of 50–75 m^3 . We note that because each box corresponded to 1 m of shoreline length, fluxes can be considered to be per meter of shoreline.

Residence times (T_r) in coral reef lagoons can be highly spatially variable and co-vary temporally with changes in circulation due to wave and wind forcing (Lowe et al. 2009; Zhang et al. 2012) or buoyancy (Herdman et al. 2015). Detailed residence time estimates can be computed with three-dimensional circulation and transport models; however, such a model does not exist for the Paopao Bay system. Instead, we estimated residence times for Paopao Bay using two methods: (1) a flushing time scale based on volume and

current speed measurements (Zimmerman 1988; Mosen et al. 2002), and (2) the difference in Ra isotope activity ratios ($^{224}\text{Ra}/^{223}\text{Ra}$ and $^{224}\text{Ra}/^{228}\text{Ra}$) between groundwater and coastal ocean surface water (Moore 2000; Street et al. 2008). For sites outside the bay and short transects comprising only a small fraction of the bay volume (FW, LW, BH, LE, and FE; Fig. 1), only the Ra-based residence time estimation method could be used because current speeds were not measured.

Flushing time, a proxy for residence time (T_r), was computed using a flushing time scale (Zimmerman 1988; Mosen et al. 2002), defined as:

$$T_r = V/Q \quad (2)$$

where V is the volume of the water body and Q is the volumetric flux of water through the system. In typical flushing time calculations, the flux is estimated either from river discharge or tidal prism. Here, the dominant flux of “new” water entering the lagoon is from wave-driven flow over the reef crest (Hench et al. 2008; Monismith et al. 2013).

To estimate water fluxes entering the lagoon during the water sampling, an acoustic Doppler current profiler (ADCP) was deployed near the reef crest ($17^\circ 28.679' \text{ S}$, $149^\circ 50.347' \text{ W}$). Current profiles were measured with a 2-MHz Nortek AquaDopp that sampled at 1 Hz and recorded as 1-minute averages. Reef crest water fluxes (q_r) were computed by integrating the product of velocities and bin heights at each height above bottom over the water column, which gives a flux that can be expressed as a volumetric flow per unit width of reef crest (Fig. 2a). Water fluxes exiting the lagoon through the reef pass (Q_p) were estimated using a similar set of ADCP velocity measurements (using a 600-kHz Teledyne RD Instruments Workhorse, deployed at $17^\circ 28.634' \text{ S}$, $149^\circ 49.492' \text{ W}$) that were sampled at 0.33 Hz and recorded as 1-minute averages. The volumetric reef pass fluxes (Fig. 2b) were estimated by multiplying the water velocities by the cross-sectional area of the pass at each ADCP bin height above bottom, as in Hench et al. (2008). The residence time of water within Paopao Bay (T_r) was then estimated using Eq. 2. This simple estimation method assumes that the volume of Paopao Bay is at steady state over the time period considered.

Activity ratio (AR) methods for estimating water residence times are based on the idea that Ra inputs from SGD have a consistent AR resulting from the hydrogeology of the aquifer. The AR measured in a coastal water body receiving SGD will be lower than that of groundwater because the shorter-lived isotope (^{224}Ra) decays faster than the longer lived one (^{223}Ra or ^{228}Ra), allowing the residence time to be calculated as follows (Moore 2000):

$$T_r = \frac{\ln(\text{AR}_{\text{co}}) - \ln(\text{AR}_{\text{gw}})}{\lambda_S - \lambda_L} \quad (3)$$

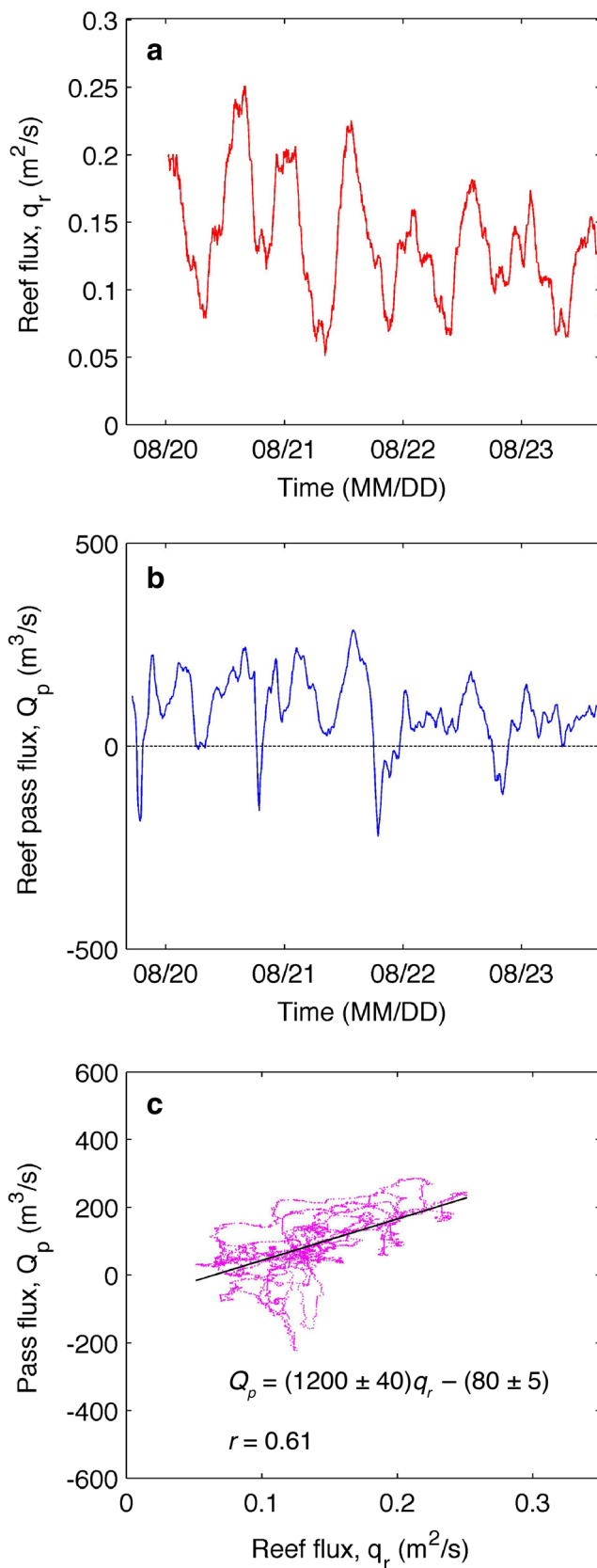


Fig. 2 Physical oceanographic data used to estimate the residence time (T_r) of Paopao Bay: **a** Unit flux of water into the system (q_{reef} , $\text{m}^2 \text{s}^{-1}$); **b** Flux of water out through the reef pass (Q_{pass} , $\text{m}^3 \text{s}^{-1}$); and **c** the correlation between the two

where AR_{co} and AR_{gw} are the ratio of the shorter-lived to the longer lived Ra isotope in coastal ocean water and discharging groundwater, respectively; and λ_S and λ_L are the decay constants (day^{-1}) of the shorter and longer lived Ra isotopes, respectively. Equation 3 assumes that Ra inputs are localized at the shoreline, although an alternate calculation (Moore et al. 2006) exists for a situation where inputs occur over a larger area, such as a well-mixed estuary. In either case, discharging groundwater and receiving coastal ocean water must have distinct ARs in order for a residence time to be calculated. If the ARs are not significantly different, only a maximum residence time estimate can be derived based on the uncertainties associated with the ARs (Street et al. 2008; Knee et al. 2008).

Unless otherwise noted, means were compared using a non-parametric Kruskal-Wallis test and differences were considered to be statistically significant if p was < 0.05 . In the case of linear regressions, a Student's t test with a significance cutoff of $p < 0.05$ was used.

Uncertainties associated with SGD fluxes were calculated using standard rules of uncertainty propagation (Taylor 1997). We used uncertainties of 5 m in the shore-perpendicular length of each box and 10 cm in the average depth of each box, and no uncertainty in the 1-m width of the box, since this parameter was assumed rather than measured. The volume of Paopao Bay can be estimated from high-resolution bathymetry data; however, uncertainty in the flushing volume (V) used in the residence time calculations arose because we could not be certain whether water exchange included the entire bay volume ($6 \times 10^7 \text{ m}^3$; Herdman et al. 2015) or only the shallow back reef area ($9 \times 10^6 \text{ m}^3$). Thus, these two values were used to represent the uncertainty range for V . The uncertainties in A_{box} and A_{gw} were approximated as the measurement uncertainty of the corresponding Ra isotope, and the uncertainty in A_{os} was estimated as the standard deviation of all the measurements averaged to generate A_{os} values. The standard deviation could not be used for A_{gw} or A_{box} because A_{gw} values were derived from a qualitative judgment about which groundwater sample best approximated the properties of the discharging groundwater endmember (see Discussion, “*Characterization of the groundwater endmember*”) and Ra activities in coastal ocean transects generally showed a decreasing trend with distance from shore; thus, measurements were not independent of each other. The uncertainty associated with T_r for Paopao Bay was estimated using standard rules of uncertainty propagation (Taylor 1997), incorporating the uncertainties in calculated values of q_r and in the regression parameters relating ocean water influxes (q_r) and outfluxes (Q_p). Because only an upper bound on residence time could be estimated using Ra isotope

ratios, no official uncertainty is associated with these residence times; however, we note that using the maximum residence time produces a minimum, or conservative, SGD estimate. Because it is likely that the residence times of these small coastal boxes are considerably less than the upper bound of 4 days, SGD could also be considerably greater than the conservative estimates.

Results

Salinity

We observed evidence of fresh to brackish groundwater in the unconfined aquifer close to shore, although coastal ocean water 0–100 m from the shoreline (Table 2) had salinity comparable to that of offshore seawater (range = 37.1–37.2, *n* = 4), indicating low freshwater input and/or extensive mixing and dilution. Salinities of coastal groundwater samples collected from shallow beach pits 0–2 m inland from the shoreline (*n* = 16) ranged from 0 to 31 with an average value (\pm standard deviation) of 8 ± 9 . At GS, groundwater salinity increased in the seaward direction during all 4 sampling events. Patterns during three of the events were similar; however, during the low tide sampling event on 8/23, salinities were considerably higher at the same distance from the shoreline (Fig. 3).

Salinities lower than the offshore average (37.2 ± 0.05 ; *n* = 4) were observed in coastal ocean water at GS and LW, as well as in Paopao Bay near the bay mouth (Fig. 4). At GS, these relatively low salinities were observed only during the high tide sampling event (8/19/08, 13:00–13:30), but not during ebb and low tide sampling events on 8/20 and 8/23 (Fig. 4). At LW, relatively low (33.3 –

36.1) salinities were observed only within 25 m of shore, and points ≥ 50 m from shore had identical salinities to offshore seawater. LW was sampled only once, during flood tide. In Paopao Bay, the three stations closest to the Bay mouth (1000 m inside, 500 m inside, and 1000 m outside the bay mouth) had salinities ranging from 36.1 to 36.4, while salinities closer to the Bay head were identical to offshore seawater. At other coastal sites, no clear evidence of freshwater inputs was observed.

Radium

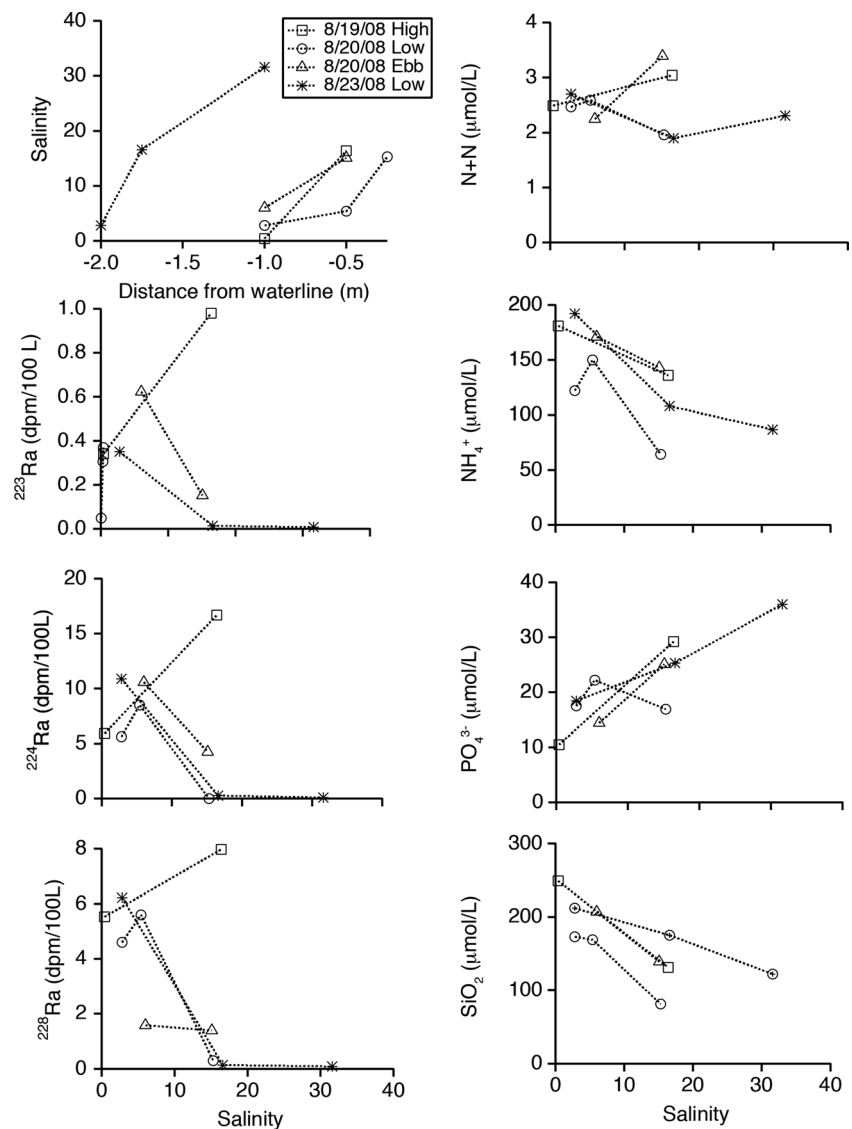
Patterns of Ra isotope activity measured in groundwater, coastal ocean water and offshore water generally supported the hypothesis that high-Ra groundwater is discharging into the coastal ocean and being progressively diluted with low-Ra seawater further offshore. The mean (\pm standard deviation) groundwater ^{223}Ra (0.43 ± 0.34 dpm/100 L) and ^{228}Ra (4.9 ± 4.3 dpm/100 L) were significantly higher than those of coastal ocean water (0.24 ± 0.13 and 1.7 ± 1.6 dpm/100 L, respectively). The difference between the mean groundwater ^{224}Ra activity (6.9 ± 5.1 dpm/100 L) and that of coastal ocean water (4.6 ± 4.1 dpm/100 L) for all sites was not statistically significant; however, within each site (FW, LW, GS, BH, and LE) groundwater ^{224}Ra activity was higher than that of the coastal ocean (Table 2). Mean ^{223}Ra , ^{224}Ra , and ^{228}Ra activities were significantly higher in coastal ocean water than in offshore water, indicating Ra inputs localized near the shore. Shore-perpendicular transects at FW, LW, GS, and LE showed steadily decreasing Ra activities from the shoreline to approximately 50–80 m offshore, with Ra activities at the last transect point similar to those of offshore samples. In Paopao Bay, the Ra-enriched zone extended to between 150 and 650 m from the bay head (Fig. 4). Notably, in Paopao Bay, high Ra activities co-occurred with seawater salinities, rather than with

Table 2 Mean ($\pm 95\%$ confidence interval) salinity, Ra isotope activities and activity ratios at each sampling site

Site	<i>n</i>		Salinity		^{223}Ra		^{224}Ra		^{228}Ra		$^{224}\text{Ra}/^{223}\text{Ra}$		$^{224}\text{Ra}/^{228}\text{Ra}$	
	GW	CO	GW	CO	(dpm/100 L)		(dpm/100 L)		(dpm/100 L)		AR		AR	
	GW	CO	GW	CO	GW	CO	GW	CO	GW	CO	GW	CO	GW	CO
FW	2	5	7.9	37.1 ± 0.1	0.64	0.2 ± 0.1	6.6	2.3 ± 1.0	3.6	0.8 ± 0.6	11.7	12 ± 9	1.1	4 ± 4
LW	2	5	2.8	36.0 ± 1.4	0.36	0.2 ± 0.1	6.3	8 ± 8	5.8	3 ± 3	21.9	28 ± 11	1.3	3 ± 2
GS	10	13	11 ± 6	36.9 ± 0.4	0.4 ± 0.2	0.2 ± 0.1	6 ± 3	4 ± 1	4.5 ± 1.8	1.7 ± 0.5	17 ± 5	16 ± 3	1.8 ± 1.1	4 ± 1
LE	1	5	1.4	37.5 ± 0.2	1.1	0.3 ± 0.1	16	4 ± 2	11	1.1 ± 0.3	14	14 ± 4	1.4	2.7 ± 1.0
BH	1	4	2.2	37.6 ± 0.2	0.46	0.25 ± 0.1	9.9	7 ± 2	15	2.8 ± 0.5	21.8	33 ± 20	0.7	2.6 ± 1.0
Paopao Bay	n/a	11	n/a	36.8 ± 0.3	n/a	0.07 ± 0.04	n/a	0.9 ± 0.9	n/a	1.2 ± 0.7	n/a	15 ± 9	n/a	1.3 ± 1.1
Offshore	n/a	4	n/a	37.2 ± 0.05	n/a	0.06 ± 0.01	n/a	0.6 ± 0.3	n/a	0.4 ± 0.1	n/a	9 ± 5	n/a	1.5 ± 0.9

GW groundwater collected from beach pits, CO coastal ocean surface water, n/a indicates that data are not available

Fig. 3 Data from tidal cycle groundwater sampling at the GS site. Groundwater was collected from a shore-perpendicular transect of 2–3 beach pits. Salinity is shown plotted against the distance inland from the waterline at the time of sample collection. Inland distances are expressed as negative numbers to distinguish them from positive offshore distances in Fig. 4. Ra and nutrient data are plotted against salinity



below-seawater salinities, indicating that the groundwater endmember causing the Ra enrichment probably had salinity close to that of seawater. At GS, where we collected multiple groundwater samples in a shore-perpendicular pit transect over the course of a tidal cycle, Ra appeared to increase with increasing salinity during the high-tide sampling event and decrease with increasing salinity during the other three sampling events at low and ebb tide (Fig. 3).

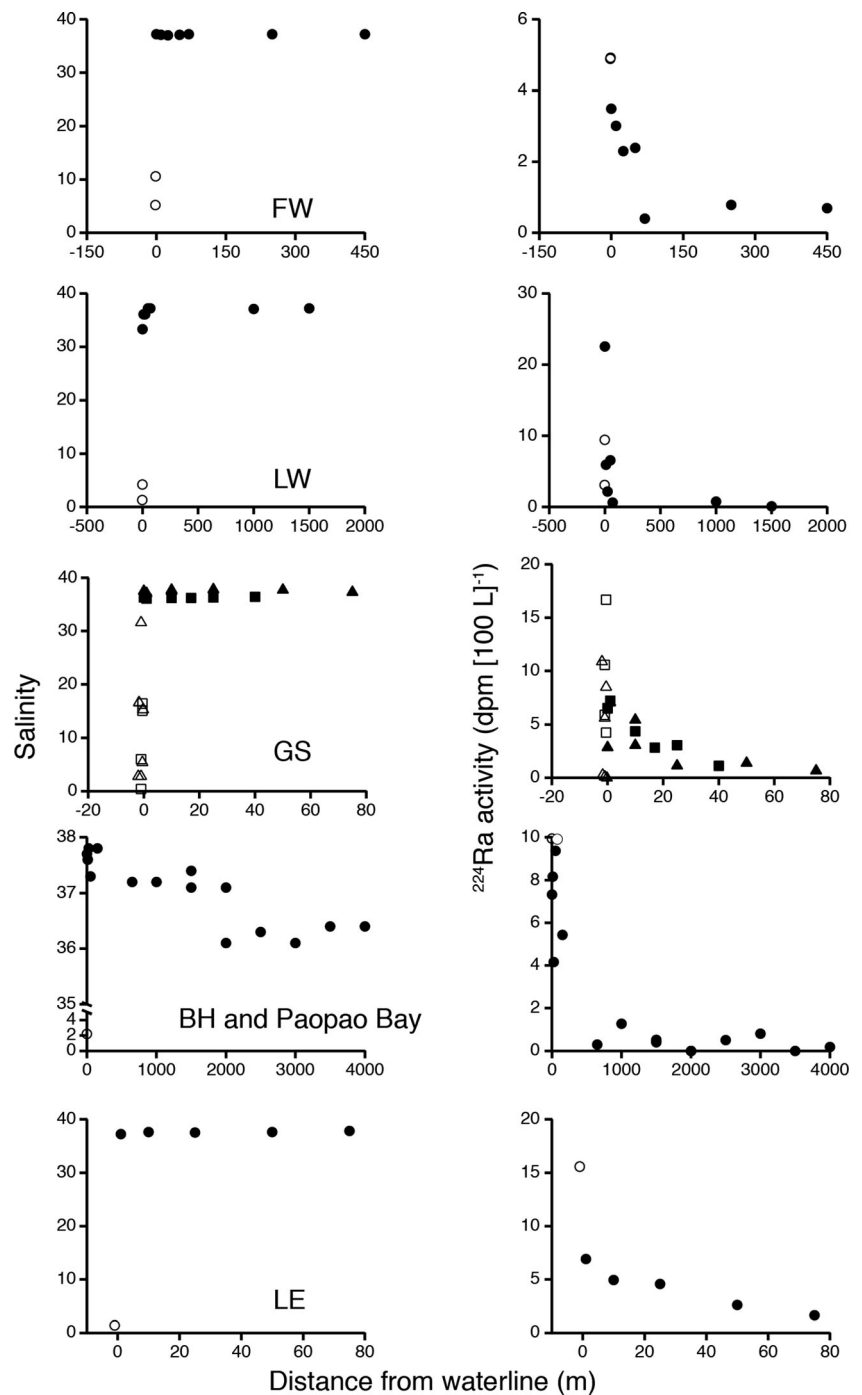
No statistically significant differences in $^{224}\text{Ra}/^{223}\text{Ra}$ or $^{224}\text{Ra}/^{228}\text{Ra}$ activity ratio were observed among the groundwater, coastal ocean, and offshore sample groups (Fig. 5), and within each coastal ocean transect site, groundwater ARs were not significantly higher than coastal ocean ARs (Table 2). This lack of statistically significant differences between the ARs of sample groups held true regardless of whether activity ratios were compared in terms of the slopes of regression lines or calculated for each sample and compared using a *t* test.

Nutrients

Average concentrations of all nutrients ($\text{N} + \text{N}$, PO_4^{3-} , NH_4^+ , and SiO_2) were significantly higher in groundwater (3.5 , 15 , 92 , and $270 \mu\text{mol L}^{-1}$, respectively) than in coastal ocean water (0.28 , 0.69 , 3.2 , and $8.4 \mu\text{mol L}^{-1}$, respectively; Fig. 5). No significant difference in the concentrations of any of these nutrients was observed between coastal ocean and offshore samples (Fig. 5) or between different coastal ocean sites (Table 3). No consistent relationships between nutrient concentrations and either distance from shore or salinity were observed along the sampling transects.

Groundwater samples from GS differed from groundwater samples from other sites (FW, LW, BH, and LE) with respect to PO_4^{3-} , NH_4^+ , and SiO_2 concentration. Average PO_4^{3-} and NH_4^+ concentrations in GS groundwater (21.6 and

Fig. 4 Variation in salinity (*left*) and ^{224}Ra activity (*right*) along shore-perpendicular transects. Positive distances are offshore and negative distances are inland of the shoreline. Open symbols indicate groundwater sampled from beach pits; closed symbols indicate coastal ocean samples. Circles indicate a single sampling event; when tidal cycle sampling was conducted, triangles indicate low or ebb tide and squares indicate high tide. ^{223}Ra and ^{228}Ra activities showed similar patterns to ^{224}Ra



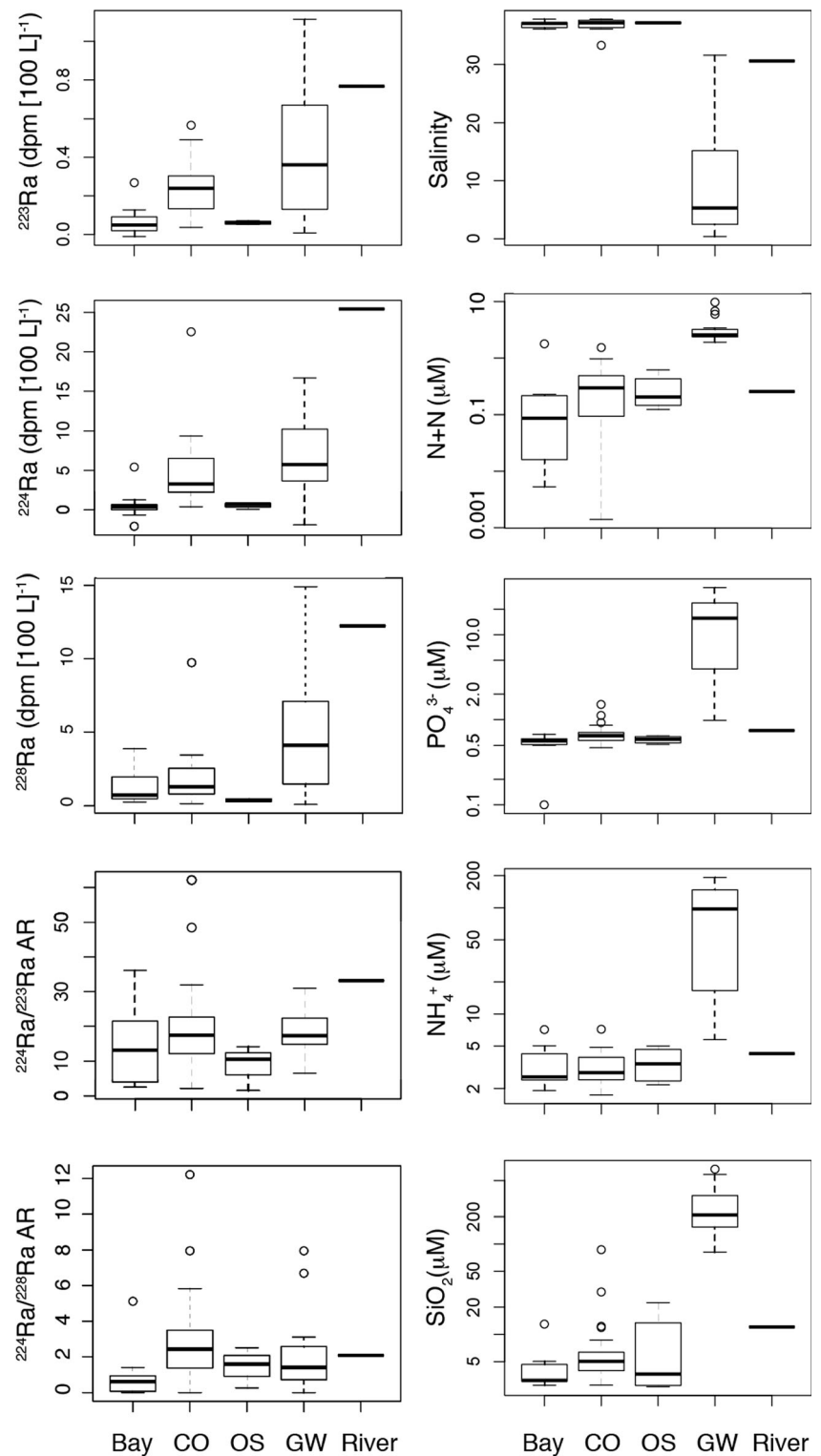
135 $\mu\text{mol L}^{-1}$, respectively) were significantly higher than in groundwater from other sites (3.17 and 19.8 $\mu\text{mol L}^{-1}$, respectively), while SiO_2 was significantly lower (166 compared to 452 $\mu\text{mol L}^{-1}$). Concentrations of NH_4^+ and SiO_2 in groundwater samples showed an inverse correlation with salinity, suggesting a fresh groundwater source (Fig. 3). In contrast, N + N concentrations did not vary in a consistent way with salinity, and PO_4^{3-} concentrations were positively correlated with salinity. These patterns, combined with the fact that groundwater N + N and PO_4^{3-} concentrations were much

higher than those in coastal ocean surface water, may indicate that recirculated seawater is equally or more enriched in these nutrients compared to fresh groundwater.

Circulation and Residence Time Estimation

Unit flux into the system (q_i) and out through the reef pass (Q_p) had a statistically significant correlation with a coefficient (r) of 0.6 (Fig. 2c). The slope of the regression line (1200 \pm 40 m) in Fig. 2c represents the total width of reef crest

Fig. 5 Box plots of salinity, Ra isotope activities and activity ratios, and nutrient concentrations by site type. Site type abbreviations are as follows: Paopao Bay (*Bay*), coastal ocean transects up to 100 m offshore (*CO*), offshore sites greater than 100 m offshore (*OS*), groundwater sampled from beach pits (*GW*) and river. Nutrient data are presented on a log scale



contributing to flow observed through the reef pass. The conceptual interpretation of this slope is that water coming onto the reef from about 600 m of reef crest on either side of the

pass is funneled into Paopao Bay and later flows out through the pass, while water flowing onto the reef more than 600 m away from the pass exchanges through other mechanisms.

Table 3 Mean ($\pm 95\%$ confidence interval) nutrient concentrations ($\mu\text{mol L}^{-1}$) at each sampling site

Site	N + N		PO ₄ ³⁻		NH ₄ ⁺		SiO ₂	
	GW	CO	GW	CO	GW	CO	GW	CO
FW	7.8	0.35 \pm 0.17	1.7	0.61 \pm 0.06	8.7	3.4 \pm 0.9	341	6 \pm 3
LW	2.5	0.11 \pm 0.07	3.3	0.84 \pm 0.44	7.0	2.4 \pm 0.4	627	26 \pm 39
GS	2.5 \pm 0.5	0.33 \pm 0.25	22 \pm 8	0.71 \pm 0.10	135 \pm 40	3.2 \pm 0.9	170 \pm 50	5.3 \pm 0.7
LE	6.8	0.40 \pm 0.24	4.8	0.59 \pm 0.11	23.1	3.4 \pm 1.2	208	6 \pm 3
BH	2.8	0.2 \pm 0.3	4.3	0.6 \pm 0.1	64.5	3.4 \pm 1.4	567	5 \pm 1
FE	n/a	0.3 \pm 0.2	n/a	0.6 \pm 0.2	n/a	2.8 \pm 1.0	n/a	9 \pm 11
Paopao Bay	n/a	0.23 \pm 0.31	n/a	0.52 \pm 0.11	n/a	3.4 \pm 0.9	n/a	5 \pm 2

GW groundwater collected from beach pits, CO coastal ocean surface water. Numbers of samples (n) are given in Table 2, except for FW, where $n = 6$

The mean reef flux (q_r) during the experiment was $0.14 \pm 0.04 \text{ m}^2 \text{ s}^{-1}$, which, according to our regression (Fig. 2c), corresponds to a total pass flux (Q_p) of $90 \pm 50 \text{ m}^3 \text{ s}^{-1}$. The mean flux thorough the reef pass measured during this same time period was $85 \pm 87 \text{ m}^3 \text{ s}^{-1}$. We note that virtually all of the uncertainty associated with these values is derived from real temporal and spatial variability in the fluxes of water in and out of the bay and from uncertainty in the regression between q_r and Q_p , not from measurement error.

To generate a residence time range for Paopao Bay, we used Eq. 2 with $Q = 90 \pm 50 \text{ m}^3 \text{ s}^{-1}$ ($8 \pm 4 \times 10^6 \text{ m}^3 \text{ d}^{-1}$) and two assumptions about the appropriate value of the bay volume, V . The first was that V was equal to $6 \times 10^7 \text{ m}^3$, the bay volume reported by Herdman et al. (2015). The second was water exchange only involved the shallow back reef area, which has a much smaller volume. Previous observational studies of circulation in the Paopao Bay system indicate that the wave-driven flow on shallow back reef and lagoon channels is distinct from the deep bay (Hench et al. 2008; Herdman et al. 2015) and that conceptually the system can be separated into two compartments: the shallow back reef and the deep bay. The back reef surface area associated with the Paopao Bay reef pass is approximately 3 km^2 with an average depth of 3 m, which gives a volume of $9 \times 10^6 \text{ m}^3$. The resulting residence time range for Paopao Bay was 18 h to 17 d. Because the flushing time estimated using this method is a linear function of the volume (Eq. 2), and the ratio of volume to residence time is incorporated in Eq. 1, SGD estimated using that equation is the same regardless of whether the large volume/long residence time or small volume/short residence time assumption is used.

²²⁴Ra/²²³Ra and ²²⁴Ra/²²⁸Ra ARs in groundwater, coastal water from short transects, and Paopao Bay displayed a high degree of variability. The 95 % confidence intervals for the ARs of groundwater and surface water from each coastal

ocean site (Table 2) were large due to the relatively small number of samples and high degree of variability within each group. Because no statistically significant differences in AR were observed between these different sample groups, specific residence times could not be calculated and the residence time range based on reef flux measurements was used for Paopao Bay. For other sites, we were able to estimate a maximum Ra-based residence time of ~ 4 d (96 h). This estimate was generated by considering how long it would take for the AR of groundwater to decrease so that its new 95 % confidence interval no longer overlapped with the original 95% confidence interval. We note that if some of the Ra present in the coastal ocean originated from a non-SGD source, such as sediments, this would introduce error into residence times calculated based on ARs and could make them invalid.

Discussion

Freshwater Inputs to Moorea's Coastal Waters

The salinity patterns we observed at coastal ocean transects (Fig. 4) suggest that fresh SGD into Moorea's coastal waters was low during the dry-season sampling period in Austral winter, but that it occurs heterogeneously in time and space. At the three sites where evidence of freshwater inputs was observed (GS, LW, and Paopao Bay near the mouth), the freshwater fraction (F_F) was calculated as:

$$F_F = 1 - \frac{S_{co}}{S_{os}} \quad (4)$$

where S_{co} is the salinity of coastal ocean water and S_{os} is the average salinity of offshore seawater measured in this study (37.2). F_F was 2.6, 5.5, and 2.5 % at GS (high tide only), LW,

and Paopao Bay mouth, respectively, and 0% at all other sites because S_{co} and S_{os} were equivalent. These are much lower fresh fractions than have been observed in the coastal waters of other volcanic islands, such as the big island of Hawai'i (Knee et al. 2010) and Jeju Island (Kim et al. 2003, 2011). At GS and LW, these fresh inputs can be assumed to come from SGD since no streams discharge at these locations. In Paopao Bay, freshwater could originate either from SGD or from the small stream discharging into the Bay head, which had a salinity of 30.6 at its mouth when sampled during this study.

The spatial and temporal patterns in salinity at GS and Paopao Bay were somewhat unexpected. Fresh SGD would generally be expected to be greater at low tide, when the hydraulic gradient between groundwater in the beach aquifer and sea surface height is steepest (e.g., de Sieyes et al. 2008); however, the opposite was observed at GS, where coastal water was observed to be fresher at high tide. Likewise, fresh inputs to Paopao Bay would be expected to be greatest near the head of the bay, which receives discharge from a stream and which would also be expected to receive the greatest amount of fresh SGD because it is furthest inland. Low salinities near the bay head, with an increasing trend in the direction of the mouth and eventually the open ocean, have been observed in Honokohau Harbor and Keauhou Bay on the big island of Hawai'i (Knee et al. 2010) and Kahana Bay on the island of O'ahu (Garrison et al. 2003). The unexpected salinity pattern in Paopao Bay may be the result of pulsed freshwater inputs followed by advective transport, tidal effects within the subterranean estuary, or a higher degree of fresh SGD occurring near the bay mouth, although no springs were observed in that area. More data collection is needed to determine whether these patterns are persistent features or whether they are specific to our study period. Additional research is also needed to account for temporal variability related to daily and fortnightly tidal cycles and seasonal variability in factors, such as wave- and thermally-driven flows, residence times, precipitation and evapotranspiration, which may influence fresh SGD.

Characterization of the Groundwater Endmember

The elevation of ^{223}Ra , ^{224}Ra , and ^{228}Ra activities in coastal ocean water collected within 100 m from shore compared to offshore water collected 250–1500 m away, combined with the relatively high activities of the three Ra isotopes in groundwater, indicate that high-Ra groundwater is discharging into the coastal ocean. Groundwater sampled from beach pits during this study was relatively fresh, with a mean salinity of 9, and a gradient of increasing groundwater salinity in the seaward direction was observed in GS pit transects (Fig. 3). These observations would suggest the discharge of fresh to brackish groundwater in the coastal zone. Evidence

of fresh or brackish inputs (i.e., surface water salinity less than 37) was observed at LW within 25 m of shore, at GS at high tide, and near the mouth of Paopao Bay. However, the freshening observed was much less than would be expected based on the salinity and Ra isotope activities of the sampled groundwater. Ra activities measured in groundwater and surface water imply that 4–6 % of water in Paopao Bay and 15–72 % of water in short coastal ocean transects is recently discharged groundwater. However, if this recently discharged groundwater had the same salinity as groundwater sampled at the corresponding beach pits, predicted coastal ocean salinities would be ~35 in Paopao Bay and 12–32 in the coastal ocean zone at other transect sites, considerably lower than the salinity ranges that we actually observed (Figs. 4 and 5).

This discrepancy implies that the groundwater sampled from the beach pits is not representative of the bulk of the discharging groundwater. A large proportion of the high-Ra SGD at these sites may consist of recirculated seawater with salinity closer to that of seawater, rather than the relatively fresh groundwater collected from beach pits. Under some circumstances, fresh SGD can occur in a layer above more saline groundwater (Robinson et al. 2007; Kuan et al. 2012); thus, by sampling shallow groundwater at the water table we may have missed the high-Ra, high-salinity layer. In addition, rapid mixing between coastal water and offshore seawater may obscure salinity gradients, making them difficult to detect with the relatively imprecise hand-held salinity meter used in this study. Previous studies of circulation in Paopao Bay (Hench et al. 2008) suggest that water flowing across the back reef may exit the reef pass over a time scale of several hours during periods of strong wave forcing and wave-driven flux. However, the presence of horizontal and vertical density stratification can drive an alternate, longer circulation pathway through the deeper portions of Paopao Bay (Herdman et al. 2015), making simple interpretations of water mass properties difficult. The implicit assumption of spatially uniform mixing within the reef and lagoon implicit in Eq. 2 also limits our ability to discern small-scale variability in residence time.

The high level of unexplained variability in Ra activities and activity ratios that we observed in groundwater and coastal ocean water indicates that Ra cycling in this system is not well understood. Variation in source Th ratios within the coastal aquifer, wave- and tide-driven flushing processes, and variation in salinity and grain size that affect Ra mobilization could all contribute to the heterogeneity observed in this study. Data from tidal cycle sampling of groundwater pits at GS (Fig. 3) showed that groundwater salinity and Ra activity at the same location and depth can vary substantially over a time scale of

hours to days. More extensive sampling, including the collection of groundwater from multiple depths within from the coastal aquifer, possibly combined with modeling, is needed to characterize the discharging groundwater endmember more precisely and enable the calculation of accurate SGD estimates.

Circulation and Residence Time

Water circulation parameters observed in this study differed from those reported previously, possibly because this study took place during the Austral winter, whereas those studies took place during the Austral summer: Dec. 2004–Feb. 2005 (Hench et al. 2008) and Dec. 2006–Feb. 2007 and Dec. 2008–Feb. 2009 (Herdman et al. 2015). Hench et al. (2008) reported a Q_p range of 500–2500 $\text{m}^3 \text{s}^{-1}$, which is much higher than the range we observed in Aug. 2008 ($85 \pm 87 \text{ m}^3 \text{s}^{-1}$), largely due to differences in wave-driven flow between the two studies. Additionally, negative Q_p values, indicating flow into the bay through the reef pass, were occasionally observed in this study (Fig. 2), but were not observed by Hench et al. (2008). The range of residence times reported in this study (18 h–7 d) represents more sluggish circulation overall and a larger absolute range of values than the range reported for Austral summer conditions (3 h–2 d; Herdman et al. 2015). More research is needed to clarify how the residence time and the relative importance of different forcing mechanisms, such as waves, tides, and buoyancy-driven mixing, vary seasonally.

The wide range of residence times reported in this and previous studies (Hench et al. 2008; Herdman et al. 2015) suggests that, even if other sources of uncertainty in SGD

calculations are reduced, it may be difficult to calculate SGD fluxes that are more precise than order-of-magnitude estimates using the mass-balance approach. This is because the residence time of water in the bay is a key component of these calculations (Eq. 2). If the bay residence time can vary by more than an order of magnitude over only a few days, it would be necessary to collect high-frequency time-series data of Ra or another natural SGD tracer, such as radon (Rn; e.g. Burnett and Dulaiova 2003, 2006; Sadat-Noori et al. 2015) in order to match up natural tracer activities with corresponding residence times and generate more precise SGD estimates.

Implications for SGD and Nutrient Loading

The higher ^{223}Ra , ^{224}Ra , and ^{228}Ra activities observed at all coastal ocean sites compared to offshore samples (Fig. 5) suggest that Ra-enriched brackish or saline groundwater is discharging into the coastal ocean. Although sediments transported by river flow (Peterson et al. 2008; Chen et al. 2010; Souza et al. 2010) or re-suspended from the seafloor (Rodellas et al. 2015) can also be a source of Ra to coastal waters, these processes are probably not the main mechanisms of Ra delivery to coastal waters in Moorea. River flow was unlikely to be a major contributor to Ra activities observed in this study because only one of the sites (Paopao Bay) had a stream discharging into it. No rainfall occurred during or immediately prior to the study period, so the stream would not have been experiencing stormflow conditions that would increase sediment transport. Additionally, our study sites do not have the high level of boat traffic that can lead to frequent sediment resuspension and associated Ra additions (Rodellas et al. 2015). Finally, differences in Ra isotope activity between

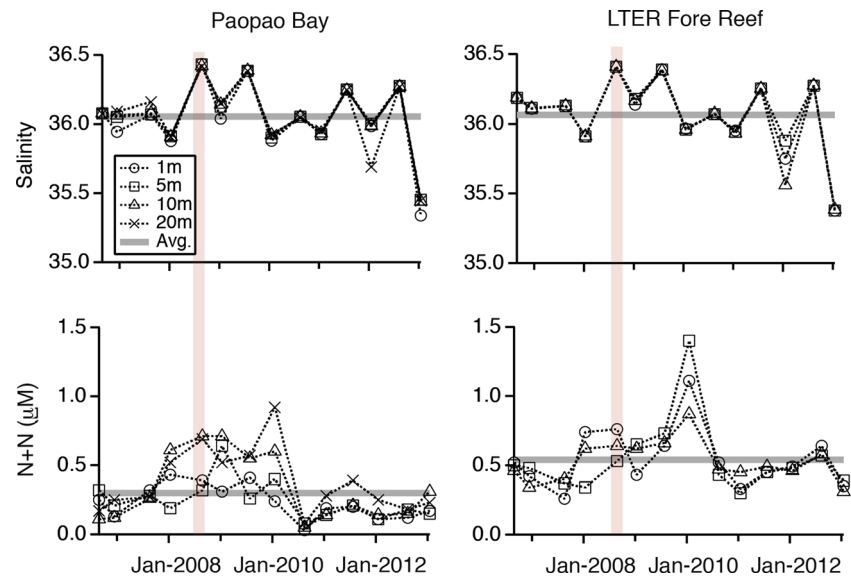
Table 4 Estimated total submarine groundwater discharge (SGD) based on Ra isotope mass balances (Eq. 1)

Site	Box volume (m^3)	Estimated residence time (days)	Estimate of total SGD* ($\text{m}^3 \text{day}^{-1}$)		
			^{223}Ra	^{224}Ra	^{228}Ra
FW	70 ± 9	≥ 4	3.1 ± 2.0	1.8 ± 0.7	1.1 ± 0.7
LW	70 ± 9	≥ 4	2.4 ± 1.6	5.1 ± 1.8	3.7 ± 2.1
GS	75 ± 9	≥ 4	1.4 ± 1.1	1.4 ± 0.6	6.5 ± 3.6
LE	75 ± 9	≥ 4	3.4 ± 2.2	3.0 ± 1.1	1.6 ± 0.9
BH	50 ± 7	≥ 4	2.2 ± 1.4	3.0 ± 1.1	3.6 ± 2.0
Paopao Bay (whole bay)	6×10^7	5–17	$0\text{--}2 \times 10^5$	$0\text{--}2 \times 10^5$	$3 \times 10^5\text{--}1 \times 10^6$
Paopao Bay (back reef only)	9×10^6	0.75–3	$0\text{--}2 \times 10^5$	$0\text{--}2 \times 10^5$	$3 \times 10^5\text{--}1 \times 10^6$

Boxes for all sites except Paopao Bay correspond to 1 m of shoreline length, so SGD fluxes can be considered to be per m shoreline

*SGD estimates for FW, LW, GS, LE, and BH are conservative (minimum) estimates because they are calculated based on maximum residence times

Fig. 6 Variation in salinity and nitrate + nitrite (N + N) concentration at several depths at the Paopao Bay (*left*) and LTER Fore Reef (*right*) sites since data collection began in 2006. The LTER Fore Reef site is located offshore of the site designated LW in this study. August 2008, when field work for this study took place, is indicated by a vertical light red bar and the mean of the data set over all depths and sampling dates is shown by a horizontal gray bar



groundwater, coastal ocean, and offshore samples were larger for ^{228}Ra , the isotope that would be least influenced by sediment inputs (Rodellas et al. 2015), than for the two shorter-lived Ra isotopes (Fig. 5, Table 2), suggesting that sediments are of limited importance as a Ra source.

Nutrient concentrations measured in beach pit groundwater samples were very high compared to those in all other sample types, but coastal ocean and offshore concentrations were indistinguishable (Fig. 5). Two possible explanations for this situation are as follows: (1) The elevated Ra levels observed in coastal ocean waters are primarily due to discharge of high-Ra, high-salinity, low-nutrient recirculated seawater rather than the high-Ra, mid-salinity, high-nutrient groundwater collected from beach pits, and (2) mixing and nutrient utilization at coastal ocean sites in Moorea are rapid, effectively diluting and erasing the SGD nutrient signature. The lack of elevated nutrient concentrations in coastal ocean transects is particularly striking when compared to other locations, such as Hawai'i (Street et al. 2008; Knee et al. 2010) where elevated nutrient concentrations and decreasing gradients in the offshore direction have been observed in coastal waters. Another contributing factor may be spatial and temporal variation in groundwater nutrient concentrations (Figs. 3 and 5), which introduce uncertainty in the characterization of the discharging groundwater endmember. If SGD into Moorea's coastal waters consists primarily of recirculated seawater, it is essential to sample this water and characterize its chemistry. Although recirculated seawater would generally be expected to have nutrient concentrations lower than fresh groundwater and/or comparable to those measured in seawater, nutrient-salinity trends at GS (Fig. 3) suggest that, at least at that site, saline groundwater/recirculated seawater may have N + N and phosphate concentrations much higher than those found in coastal or offshore seawater. Additional sampling to characterize the

Ra activities and nutrient concentrations of the discharging saline groundwater endmember is necessary to resolve this issue.

Estimating SGD and associated nutrient fluxes for Paopao Bay and the other coastal ocean sites where Ra was measured (FW, LW, GS, and LE) was difficult because (1) the groundwater sampled from beach pits was not representative of the total discharging groundwater in terms of combination of Ra activity and salinity, and, thus, may not have been representative in terms of nutrient concentrations either, and (2) residence times could not be determined precisely. To generate tentative first order estimates of SGD into Paopao Bay and segments of Moorea's open (non-bay) coastline, we assumed that the salinity and Ra activities of the discharging groundwater endmember could be best approximated by the groundwater sample collected from the most inland pit at GS during low tide on 8/19/08 (Fig. 3). This sample had the relatively high salinity (16.4) and high Ra isotope activities (0.98, 16.7, and 8.0 dpm [100 L] $^{-1}$ for ^{223}Ra , ^{224}Ra and ^{228}Ra , respectively) that would be expected in a groundwater endmember containing a higher proportion of recirculated seawater. However, if the Ra isotope activities of the discharging groundwater endmember were actually higher/lower than those in this sample, using it as the endmember would result in an overestimation/underestimation of SGD. A Ra-based maximum residence time of 4 days, corresponding to a conservative SGD estimate, was used for all open coastline sites, and a residence time range of 5–17 days (along with a volume of $6 \times 10^7 \text{ m}^3$) was used for Paopao Bay. The lower bound on residence time cited earlier (18 hours) corresponds to a smaller estimate of the bay flushing volume, and, when used in combination with that volume in SGD calculations, produces the same SGD estimate as the larger volume/longer residence time assumption. This resulted in the following tentative,

conservative estimates of total SGD: 1.1 ± 0.7 – $6.5 \pm 3.6 \text{ m}^3 \text{ day}^{-1}$ per meter of shoreline for the open shoreline sites (FW, LW, GS, and LE) and 0 – $1 \times 10^6 \text{ m}^3 \text{ day}^{-1}$ into Paopao Bay (Table 4).

These estimates are within the range reported for other volcanic islands with coral reefs (Table 1); however, that range is very wide due to the uncertainties in residence time and groundwater Ra activities, and more precise estimates must be made to determine how the degree of SGD influence on Moorea compares to other islands. Since nutrient concentrations in sampled groundwater were much higher than in coastal ocean water (Table 3), even relatively low SGD could contribute ecologically important nutrient subsidies (e.g., Shellenbarger et al. 2006). However, the nutrient concentrations of the discharging groundwater endmember at each site must be better characterized in order to estimate those subsidies. In particular, the variation in nutrient concentrations with salinity as groundwater flows through the subterranean estuary should be investigated.

Limitations and Recommendations for Future Study

Although we present tentative estimates of SGD based on reasonable assumptions, Ra and salinity balances for the coastal ocean sites included in this study revealed that the groundwater sampling we conducted was not sufficient to characterize the discharging groundwater endmember and precluded precise estimation of SGD. In future work, multi-level piezometer sampling (e.g., Charette and Allen 2006) should be used to delineate vertical variability in salinity, Ra isotope activities and nutrient concentrations in coastal groundwater. This variability may be considerable due to flow line compression as groundwater approaches the shoreline. Rock underlying beach sand at the study sites may complicate or prevent multi-level piezometer sampling. If conditions make it impossible to determine the chemistry of the discharging groundwater endmember, alternate approaches, such as water balance or numerical modeling, should be considered for the determination of SGD.

We were also unable to use Ra isotope ARs to calculate precise coastal residence times because no significant differences in AR between groundwater and surface water were observed, and, even if they had been, the groundwater we were able to collect may not have been representative of the groundwater that was adding Ra to the coastal ocean. The different Ra/salinity makeup of the groundwater we sampled and the saline groundwater that we hypothesize is discharging is most likely not due to geological heterogeneity, because Moorea has similar rock types throughout the island (Williams 1933). Rather, it may be caused by heterogeneity in salinity and Ra isotope activities within the subterranean estuary related to flushing by waves and tides (e.g., Robinson et al. 2007; Gonnee et al. 2008). It is possible that, if multi-

level piezometer sampling succeeded in identifying the discharging groundwater endmember, that endmember might have a distinct AR from coastal seawater and Ra-based residence times could be calculated. However, given the high level of variability in AR we observed in all sample groups, we recommend using an alternate method if residence times are required for sections of Moorea's coastal waters in the future.

In addition to the limitations mentioned above, it is important to keep in mind that, because the field sampling took place during a 1-week period in August 2008, it represents a single snapshot in time. Both the quantity and quality of SGD can vary with daily and fortnightly tidal cycles (Taniguchi et al. 2002; De Sieyes et al. 2008), as well as with seasonal variations in wave set-up, precipitation and other factors (Kelly and Moran 2002; Michael et al. 2005; Oliveira et al. 2006). Bi-annual monitoring in Paopao Bay and LTER1 since 2006 has shown considerable seasonal and interannual variability in salinity, and nitrate + nitrite (N + N) concentration. The period of our field sampling in August 2008 had higher than average salinity and N + N concentration compared to the entire 2006–2013 monitoring period (Fig. 6). Future SGD studies on Moorea should focus on discerning patterns of temporal variability in SGD quantity and quality so that annual estimates of SGD and the associated nutrient loading to coral reefs can be made with confidence.

Conclusions

Elevated Ra isotope activities in Paopao Bay and nearby coastal ocean transects on Moorea indicated that SGD occurs in these locations. Conservative estimates of SGD at coastal ocean transects ranged from 1.1 ± 0.7 to $6.5 \pm 3.6 \text{ m}^3 \text{ d}^{-1}$ per meter of shoreline, and estimates of SGD into Paopao Bay ranged from 0 to $1 \times 10^6 \text{ m}^3 \text{ d}^{-1}$. At FW, BH, and FE, no discernible freshening of coastal seawater was observed, indicating that almost all SGD is recirculated seawater. At GS, LW and near the mouth of Paopao Bay, salinities lower than the average offshore salinity were observed. At GS and LW, this freshwater must come from SGD because no streams are present, although in Paopao Bay, a stream source cannot be ruled out. More research is needed to characterize the discharging groundwater endmember and determine the importance of SGD to coastal ocean nutrient budgets in this area.

Acknowledgments We thank Ellen Gray and other members of the Paytan lab group (University of California, Santa Cruz) for help collecting and analyzing water samples for this study. Two anonymous reviewers provided comments that led to the improvement of the manuscript. This research was funded by a small grant from the NSF Moorea Coral Reef Long-Term Ecological Research (LTER) program (OCE-0417412) to AP.

References

- Baker, D.M., S.E. MacAvoy, and K. Kim. 2007. Relationship between water quality, $\delta^{15}\text{N}$, and aspergillosis of Caribbean Sea fan corals. *Marine Ecology Progress Series* 343: 123–130.
- Basu, A.R., S.B. Jacobson, R.J. Poreda, C.B. Dowling, and P.K. Aggarwal. 2001. Large groundwater strontium flux to the oceans from the Bengal Basin and the marine strontium isotope record. *Science* 293: 1470–1473.
- Blanco, A.C., A. Watanabe, K. Nadaoka, S. Motooka, E.C. Herrera, and T. Yamamoto. 2011. Estimation of nearshore groundwater discharge and its potential effects on a fringing coral reef. *Marine Pollution Bulletin* 62: 770–785.
- Boutillier, S., and T. Duane. 2006. Land use planning to promote marine conservation of coral reef ecosystems in Moorea, French Polynesia. University of California, Berkeley, Department of Landscape Architecture and Environmental Planning, Pacific Rim Research Program. Accessed Aug. 5, 2014 at <http://escholarship.org/uc/item/10f3q5p4>.
- Bruno, J.F., L.E. Petes, C.D. Harvell, and A. Hettinger. 2003. Nutrient enrichment can increase the severity of coral disease. *Ecology Letters* 6: 1056–1061.
- Burnett, W.C., and H. Dulaiova. 2003. Estimating the dynamics of groundwater input into the coastal zone via continuous radon-222 measurements. *Journal of Environmental Radioactivity* 69: 21–35.
- Burnett, W.C., and H. Dulaiova. 2006. Radon as a tracer of submarine groundwater discharge into a boat basin in Donnalucata, Sicily. *Continental Shelf Research* 26: 862–873.
- Burnett, W.C., M. Taniguchi, and J. Oberdorfer. 2001. Measurement and significance of the direct discharge of groundwater into the coastal zone. *Journal of Sea Research* 46: 109–116.
- Burnett, W.C., G. Wattayakorn, M. Taniguchi, H. Dulaiova, P. Sojisuporn, S. Rungsupa, and T. Ishitobi. 2007. Groundwater-derived nutrient inputs to the Upper Gulf of Thailand. *Continental Shelf Research* 27: 176–190.
- Charette, M.A., and M.C. Allen. 2006. Precision ground water sampling in coastal aquifers using a direct-push, shielded-screen well-point system. *Groundwater Monitoring and Remediation* 26(2): 87–93.
- Chen, W., Q. Liu, C.-A. Huh, M. Dai, and Y.-C. Miao. 2010. Signature of the Mekong River plume in the western South China Sea revealed by radium isotopes. *Journal of Geophysical Research* 115: C12002.
- Coles, S.L., and P.L. Jokiel. 1992. Effects of salinity on coral reefs. In *Pollution in tropical aquatic systems*, eds. D. Connell, and D. Hawker, 147–166. Boca Raton: CRC Press.
- Crotwell, A.M., and W.S. Moore. 2003. Nutrient and radium fluxes from submarine groundwater discharge to Port Royal Sound, South Carolina. *Aquatic Geochemistry* 9: 191–208.
- De Sieyes, N.R., K.M. Yamahara, B.A. Layton, E.H. Joyce, and A.B. Boehm. 2008. Submarine discharge of nutrient-enriched fresh groundwater at Stinson Beach, California is enhanced during neap tides. *Limnology and Oceanography* 53: 1434–1445.
- Duarte, T.K., H.F. Hemond, D. Frankel, and S. Frankel. 2006. Assessment of submarine groundwater discharge by handheld aerial infrared imagery: case study of Kaloko fishpond and bay, Hawai'i. *Limnology and Oceanography: Methods* 4: 227–236.
- Fabricius, K.E. 2005. Effects of terrestrial runoff on the ecology of corals and coral reefs: review and synthesis. *Marine Pollution Bulletin* 50: 125–146.
- Freeze, R.A., and J.A. Cherry. 1979. *Groundwater*. Englewood Cliffs, NJ, USA: Prentice-Hall.
- Garcia-Solsona, E., J. Garcia-Orellana, P. Masqué, and H. Dulaiova. 2008. Uncertainties associated with ^{223}Ra and ^{224}Ra measurements in water via a delayed coincidence counter (RaDeCC). *Marine Chemistry* 109: 198–219.
- Garrison, G., C.R. Glenn, and G.R. McMurtry. 2003. Measurement of submarine groundwater discharge in Kahana Bay, O'ahu, Hawai'i. *Limnology and Oceanography* 48: 920–928.
- Giambelluca, T.W., Q. Chen, A.G. Frazier, J.P. Price, Y.-L. Chen, P.-S. Chu, J.K. Eischeid, and D.M. Delparte. 2013. Online rainfall atlas of Hawai'i. *Bulletin of the American Meteorological Society* 94: 313–316.
- Gonneea, M.E., P.J. Morris, H. Dulaiova, and M.A. Charette. 2008. New perspectives on radium behavior within a subterranean estuary. *Marine Chemistry* 109: 250–267.
- Hench, J.L., J.J. Leichter, and S.G. Monismith. 2008. Episodic circulation and exchange in a wave-driven coral reef and lagoon system. *Limnology and Oceanography* 53: 2681–2694.
- Herdman, L.M., J.L. Hench, and S.G. Monismith. 2015. Heat balances and thermally-driven lagoon-ocean exchanges on a tropical coral reef system (Moorea, French Polynesia). *Journal of Geophysical Research, Oceans* 120: 1233–1252.
- Hildenbrand, A., C. Marlin, A. Conroy, P.Y. Gillot, A. Filly, and M. Massault. 2005. Isotopic approach of rainfall and groundwater circulation in the volcanic structure of Tahiti-Nui (French Polynesia). *Journal of Hydrology* 302: 187–208.
- Hwang, D.-W., Y.-W. Lee, and G. Kim. 2005. Large submarine groundwater discharge and benthic eutrophication in Bangdu Bay on volcanic Jeju Island, Korea. *Limnology and Oceanography* 50: 1393–1403.
- Institut Statistique de Polynésie Française (ISPF). 2015. Tableau II Population des communes et communes associées de Polynésie française. Retrieved Sept. 4, 2015.
- Ji, T., J. Du, W.S. Moore, G. Zhang, N. Su, and J. Zhang. 2013. Nutrient inputs to a lagoon through submarine groundwater discharge: the case of Laoye Lagoon, Hainan, China. *Journal of Marine Systems* 111–112: 253–262.
- Johnson, A. G. 2012. A water-budget model and estimates of groundwater recharge for Guam. U.S. Geological Survey Scientific Investigation Report 2012–5028, 53 p.
- Johnson, A.G., C.R. Glenn, W.C. Burnett, R.N. Peterson, and P.G. Lucey. 2008. Aerial infrared imaging reveals large nutrient-rich groundwater inputs to the ocean. *Geophysical Research Letters* 35: L15606.
- Jokiel, P.L. 2004. Temperature stress and coral bleaching. In *Coral health and disease*, eds. E. Rosenberg, and Y. Loya, 401–425. New York: Springer.
- Kelly, R.P., and S.B. Moran. 2002. Seasonal changes in groundwater input to a well-mixed estuary estimated using radium isotopes and implications for coastal nutrient budgets. *Limnology and Oceanography* 47: 1796–1807.
- Kim, G., and P.W. Swarzenski. 2010. Submarine groundwater discharge (SGD) and associated nutrient fluxes to the coastal ocean. In *Carbon and nutrient fluxes in continental margins*, eds. K.-K. Liu, and et al. Berlin Heidelberg: Springer-Verlag.
- Kim, G., K.-K. Lee, K.-S. Park, D.-W. Hwang, and H.-S. Yang. 2003. Large submarine groundwater discharge (SGD) from a volcanic island. *Geophysical Research Letters* 30: 2098.
- Kim, G., J.-S. Kim, and D.-W. Hwang. 2011. Submarine groundwater discharge from oceanic islands standing in oligotrophic oceans: implications for global biological production and organic carbon fluxes. *Limnology and Oceanography* 56: 673–682.
- Knee, K.L., B.A. Layton, J.H. Street, A.B. Boehm, and A. Paytan. 2008. Sources of nutrients and fecal indicator bacteria to nearshore waters on the north shore of Kaua'i (Hawai'i, USA). *Estuaries and Coasts* 31: 607–622.
- Knee, K.L., J.H. Street, E.E. Grossman, A.B. Boehm, and A. Paytan. 2010. Nutrient inputs to the coastal ocean from submarine groundwater discharge in a groundwater-dominated system: relation to land use (Kona coast, Hawai'i, USA). *Limnology and Oceanography* 55: 1105–1122.

- Kroeger, K.D., P.W. Swarzenski, W.J. Greenwood, and C. Reich. 2007. Submarine groundwater discharge to Tampa Bay: nutrient fluxes and biogeochemistry of the coastal aquifer. *Marine Chemistry* 104: 85–97.
- Kuan, W.K., G. Jin, P. Xin, C. Robinson, B. Gibbes, and L. Li. 2012. Tidal influence on seawater intrusion in unconfined coastal aquifers. *Water Resources Research* 48: W02502.
- Leichter, J.J., A.L. Alldredge, G. Bernardi, A.J. Brooks, C.A. Carlson, R.C. Carpenter, P.J. Edmunds, M.R. Fewings, K.M. Hanson, J.L. Hench, et al. 2013. Biological and physical interactions on a tropical island coral reef: transport and retention processes on Moorea, French Polynesia. *Oceanography* 26: 52–63. doi:10.5670/oceanog.2013.45.
- Lin, I.-T., C.-H. Wang, S. Lin, and Y.-G. Chen. 2011. Groundwater-seawater interactions off the coast of southern Taiwan: evidence from environmental isotopes. *Journal of Asian Earth Sciences* 41: 250–262.
- Lowe, R.J., J.L. Falter, S.G. Monismith, and M.J. Atkinson. 2009. A numerical study of circulation in a coastal reef-lagoon system. *Journal of Geophysical Research, Oceans* 114: C06022.
- Macdonald, G.A., A.T. Abbott, and F.L. Peterson. 1983. *Volcanoes in the sea: the geology of Hawaii*. Honolulu: University of Hawaii Press.
- Matson, E.A. 1993. Nutrient flux through soils and aquifers to the coastal zone of Guam (Mariana Islands). *Limnology and Oceanography* 38: 361–371.
- McCook, L.J., J. Jompa, and G. Diaz-Pulido. 2001. Competition between corals and algae on coral reefs: a review of evidence and mechanisms. *Coral Reefs* 19: 400–417.
- Michael, H.A., A.E. Mulligan, and C.F. Harvey. 2005. Seasonal oscillations in water exchange between aquifers and the coastal ocean. *Nature* 436: 1145–1148.
- Monismith, S.G., L.M.M. Herdman, S.H. Ahmerkamp, and J.L. Hench. 2013. Wave transformation and wave-driven flow across a steep coral reef. *Journal of Physical Oceanography* 43: 1356–1379.
- Monsen, N.E., J.E. Cloern, L.V. Lucas, and S.G. Monismith. 2002. A comment on the use of flushing time, residence time, and age as transport time scales. *Limnology and Oceanography* 47: 1545–1553.
- Montluçon, D., and S.A. Sañudo-Wilhelmy. 2001. Influence of net groundwater discharge on the chemical composition of a coastal environment: Flanders Bay, Long Island, New York. *Environmental Science and Technology* 35: 480–486.
- Moore, W.S. 2000. Determining coastal mixing rates using radium isotopes. *Continental Shelf Research* 20: 1993–2007.
- Moore, W.S., J.O. Blanton, and S.B. Joye. 2006. Estimates of flushing times, submarine groundwater discharge, and nutrient fluxes to Okatee Estuary, South Carolina. *Journal of Geophysical Research: Oceans* 111(C9). doi:10.1029/2005JC003041.
- Moorea Coral Reef LTER. 2014. Gump station meteorological data, ongoing since 2006. knb-lter-mcr.9.37 (<http://metacat.lternet.edu/knb/metacat/knb-lter-mcr.9.37/lter>).
- Neall, V.E., and S.A. Trewick. 2008. The age and origin of the Pacific islands: a geological overview. *Philosophical Transactions of the Royal Society of London B* 363(1508): 3298–3308.
- Null, K.A., N.T. Dimova, K.L. Knee, B.K. Esser, P.W. Swarzenski, M.J. Singleton, M. Stacey, and A. Paytan. 2012. Submarine groundwater discharge-derived nutrient loads to San Francisco Bay: implications to future ecosystem changes. *Estuaries and Coasts* 35: 1299–1315.
- Null, K.A., K.L. Knee, E.D. Crook, N.R. de Sieyes, M. Rebollo-Vieyra, L. Hernández-Terrones, and A. Paytan. 2014. Composition and fluxes of submarine groundwater along the Caribbean coast of the Yucatan Peninsula. *Continental Shelf Research* 77: 38–50.
- Oliveira, J., P. Costa, and E.S. Braga. 2006. Seasonal variations of ²²²Rn and SGD fluxes to Ubatuba embayments, São Paulo. *Journal of Radioanalytical and Nuclear Chemistry* 269: 689–695.
- Pasturel, J. 1993. La climatologie des îles. Atlas de la Polynésie Française. O.R.S.T.O.M. éditions: planches 42–43.
- Paytan, A., G.G. Shellenbarger, J.H. Street, M.E. Gonneea, K. Davis, M.B. Young, and W.S. Moore. 2006. Submarine groundwater discharge: an important source of new inorganic nitrogen to coral reef ecosystems. *Limnology and Oceanography* 51: 343–348.
- Peng, T.-R., C.-T.A. Chen, C.-H. Wang, J. Zhang, and Y.-J. Lin. 2008. Assessment of terrestrial factors controlling submarine groundwater discharge in water shortage and highly deformed island of Taiwan, Western Pacific Ocean. *Journal of Oceanography* 64: 323–337.
- Peterson, R.N., W.C. Burnett, M. Taniguchi, J. Chen, I.R. Santos, and T. Ishitobi. 2008. Radon and radium isotope assessment of submarine groundwater discharge in the Yellow River delta, China. *Journal of Geophysical Research* 113: C09021.
- Peterson, R.N., W.C. Burnett, C.R. Glenn, and A.G. Johnson. 2009. Quantification of point-source groundwater discharges to the ocean from the shoreline of the Big Island, Hawaii. *Limnology and Oceanography* 54: 890–904.
- Povinec, P.P., W.C. Burnett, A. Beck, H. Bokuniewicz, M. Charette, M.E. Gonneea, M. Groening, T. Ishitobi, Y. Kontar, L.L. Wee Kwong, D.E.P. Marie, W.S. Moore, J.A. Oberdorfer, R. Peterson, R. Ramessur, J. Rapaglia, T. Stieglitz, and Z. Top. 2012. Isotopic, geochemical and biogeochemical investigation of submarine groundwater discharge: IAEA-UNESCO intercomparison exercise at Mauritius Island. *Journal of Environmental Radioactivity* 104: 24–45.
- Resh, V.H., M. Moser, and M. Poole. 1999. Feeding habits of some freshwater fishes in streams of Moorea, French Polynesia. *Annals of Limnology* 35: 205–210.
- Robinson, C., L. Li, and D.A. Barry. 2007. Effect of tidal forcing on a subterranean estuary. *Advances in Water Resources* 30: 851–865.
- Rodellas, V., J. Garcia-Orellana, P. Masqué, and J.S. Font-Muñoz. 2015. The influence of sediment sources on radium-derived estimates of Submarine Groundwater Discharge. *Marine Chemistry* 171: 107–117.
- Sadat-Noori, M., I.R. Santos, C.J. Sanders, L.M. Sanders, and D.T. Maher. 2015. Groundwater discharge into an estuary using spatially distributed radon time series and radium isotopes. *Journal of Hydrology* 528: 703–719.
- Senal, M.I.S., G.S. Jacinto, M.L. San Diego-McGlone, F. Siringan, P. Zamora, L. Soria, M.B. Cardenas, C. Villanoy, and O. Cabrera. 2011. Nutrient inputs from submarine groundwater discharge on the Santiago reef flat, Boliano, Northwestern Philippines. *Marine Pollution Bulletin* 63: 195–200.
- Serafini, J., J.P. Barriot, and L. Sichoix. 2014. The evolution of precipitable water and precipitation over the island of Tahiti from hourly to seasonal periods. *International Journal of Remote Sensing* 35(18): 6687–6707.
- Shellenbarger, G.G., S.G. Monismith, A. Genin, and A. Paytan. 2006. The importance of submarine groundwater discharge to the near-shore nutrient supply in the Gulf of Aqaba (Israel). *Limnology and Oceanography* 51: 1876–1886.
- Souza, T.A., J.M. Godoy, M.L.D.P. Godoy, I. Moreira, Z.L. Carvalho, M.S.M.B. Salomão, and C.E. Rezende. 2010. Use of multitracers for the study of water mixing in the Paraíba do Sul River estuary. *Journal of Environmental Radioactivity* 101: 564–570.
- Spalding, M.D., C. Ravilious, and E.P. Green. 2001. *World atlas of coral reefs. Prepared at the UNEP World Conservation Monitoring Centre*. Berkeley and Los Angeles: University of California Press 424 pp.
- Street, J.H., K.L. Knee, E.E. Grossman, and A. Paytan. 2008. Submarine groundwater discharge and nutrient addition to the coastal zone and coral reefs of leeward Hawai'i. *Marine Chemistry* 109: 355–376.
- Su, N., J. Du, W.S. Moore, S. Liu, and J. Zhang. 2011. An examination of groundwater discharge and the associated nutrient fluxes into the

- estuaries of eastern Hainan Island, China, using ^{226}Ra . *Science of the Total Environment* 409: 3909–3918.
- Sutherland, K. Patterson, S. Shaban, J.L. Joiner, J.W. Porter, and E.K. Lipp. 2011. Human pathogen shown to cause disease in the threatened Elkhorn coral *Acropora palmata*. *PLoS One* 6: e23468.
- Taniguchi, M., W.C. Burnett, J.E. Cable, and J.V. Turner. 2002. Investigation of submarine groundwater discharge. *Hydrological Processes* 16: 2115–2129.
- Taniguchi, M., T. Ishitobi, and K.-I. Saeki. 2005. Evaluation of space-time distributions of submarine groundwater discharge. *Groundwater* 43: 336–342.
- Taniguchi, M., W.C. Burnett, H. Dulaiova, F. Siringan, J. Foronda, G. Wattayakorn, S. Rungsupa, E.A. Kontar, and T. Ishitobi. 2008. Groundwater discharge as an important land-sea pathway into Manila Bay, Philippines. *Journal of Coastal Research* 24: 15–24.
- Taylor, J.R. 1997. *An introduction to error analysis*, 2nd edn, 160–168. Sausalito: University Science Books.
- Van Dam, J.W., A.P. Negri, S. Uthicke, and J.F. Mueller. 2011. Chemical pollution on coral reefs: exposure and ecological effects. In *Ecological impacts of toxic chemicals*, eds. Francisco Sanchez-Bayo et al., 187–211. Amsterdam: Bentham Books.
- Voss, J.D., and L.L. Richardson. 2006. Nutrient enrichment enhances black band disease progression in corals. *Coral Reefs* 25: 569–576.
- Washburn, L. 2014. MCR LTER: Coral Reef: Ocean currents and biogeochemistry: salinity, temperature and current at CTD and ADCP mooring FOR01 from 2004 ongoing. knb-lter-mcr.30.26. <http://metacat.lternet.edu/knb/metacat/knb-lter-mcr.30.26/lter>.
- Williams, H. 1933. Geology of Tahiti, Moorea, and Maiao. Bernice P. Bishop Museum Bulletin 105. Honolulu, Hawaii, The Museum.
- Won, J.H., J.Y. Lee, J.W. Kim, and G.W. Koh. 2006. Groundwater occurrence on Jeju Island, Korea. *Hydrogeology Journal* 14(4): 532–547.
- Zhang, Z., J. Falter, R. Lowe, and G. Ivey. 2012. The combined influence of hydrodynamic forcing and calcification on the spatial distribution of alkalinity in a coral reef system. *Journal of Geophysical Research, Oceans* 117: C04034.
- Zimmerman, J.T.F. 1988. Estuarine residence times. In *Hydrodynamics of Estuaries. Vol. 1*, ed. B. Kjerfve, 75–84. Boca Raton: CRC Press.